



Rapid sea level rise and ice sheet response to 8,200-year climate event

T. M. Cronin,¹ P. R. Vogt,² D. A. Willard,¹ R. Thunell,³ J. Halka,⁴ M. Berke,¹ and J. Pohlman⁵

Received 24 July 2007; revised 27 August 2007; accepted 4 September 2007; published 24 October 2007.

[1] The largest abrupt climatic reversal of the Holocene interglacial, the cooling event 8.6–8.2 thousand years ago (ka), was probably caused by catastrophic release of glacial Lake Agassiz-Ojibway, which slowed Atlantic meridional overturning circulation (AMOC) and cooled global climate. Geophysical surveys and sediment cores from Chesapeake Bay reveal the pattern of sea level rise during this event. Sea level rose ~14 m between 9.5 to 7.5 ka, a pattern consistent with coral records and the ICE-5G glacio-isostatic adjustment model. There were two distinct periods at ~8.9–8.8 and ~8.2–7.6 ka when Chesapeake marshes were drown as sea level rose rapidly at least ~12 mm yr⁻¹. The latter event occurred after the 8.6–8.2 ka cooling event, coincided with extreme warming and vigorous AMOC centered on 7.9 ka, and may have been due to Antarctic Ice Sheet decay. **Citation:** Cronin, T. M., P. R. Vogt, D. A. Willard, R. Thunell, J. Halka, M. Berke, and J. Pohlman (2007), Rapid sea level rise and ice sheet response to 8,200-year climate event, *Geophys. Res. Lett.*, 34, L20603, doi:10.1029/2007GL031318.

1. Introduction

[2] Rising sea level due in part to mass balance changes in the Greenland and Antarctic Ice Sheets is of great concern [Miller and Douglas, 2004; Shepherd and Wingham, 2007], especially given new evidence for rapid ice discharge [Howat et al., 2007] and reassessment of ice sheet timescales due to subglacial processes and ice sheet dynamics [Truffer and Fahnestock, 2007]. But the rates and patterns of sea level rise during past abrupt climate events are poorly known [Alley et al., 2005]. One such event – the abrupt cooling ~8.6 to 8.2 ka [Alley et al., 1997; Rohling and Pälike, 2005] caused by glacial Lakes Agassiz-Ojibway drainage [Barber et al., 1999; Teller et al., 2002] had immediate large-scale atmospheric impacts [Cuffey and Clow, 1997; Haug et al., 2001], cooled and freshened North Atlantic surface waters, and slowed AMOC, before a strong warming trend resumed ~7.9 ka [Ellison et al., 2006]. Reconstruction of sea level rise during the early part of the Holocene interglacial can be particularly insightful because by ~9 ka, roughly 80% of the total continental ice from the Last Glacial Maximum (LGM) had melted, and sea level was about 20–25 m below that of the present day.

[3] We examined relative sea level (RSL) using geophysical and sediment core data obtained on cruises of the *R/V Marion-Dufresne* in 1999 [Cronin, 2000] and 2003 [Laj, 2005] to Chesapeake Bay, the largest estuary in the United States (Figure 1, inset). Chesapeake Bay is ideal for reconstructing Holocene sea level due to its excellent chronology [Cronin et al., 2005; Willard et al., 2005], firm estimates of regional post-glacial isostatic adjustment (GIA) [Peltier, 1996] (~1.0 mm yr⁻¹), negligible vertical tectonic movement, and multiple sea level indicators. Coring sites were selected using single-channel seismic reflection and 3.5 kHz surveys, 2–15 kHz CHIRP subbottom profiles, and 100 kHz sidescan sonar mosaics, and results from short cores taken on prior cruises.

2. Chesapeake Bay Sea Level Record

[4] The thick [>25 m] Holocene sequence consists of fluvial, coastal, and estuarine units deposited above the Cape Charles erosion surface (CCES), which was excavated to ca. 50–55 mbsl during the LGM (Figure 1a) [Colman et al., 1990; Vogt et al., 2000]. Figure 1b shows the stratigraphy and depositional environments for each core projected onto an idealized west-to-east cross section and three RSL positions discussed below. The transect of cores records the time-transgressive fluvial-marine transition in three distinct regions – the deep channel, the eastern marsh near Pocomoke Sound, and the oyster reefs on the west side of the bay. Stratigraphic units are distinguished on the basis of CHIRP profiles, lithology, magnetic susceptibility (MS), micropaleontology, and dated by AMS radiocarbon dates (¹⁴C dates in the auxiliary material,¹ proxy data available at <http://www.ncdc.noaa.gov/paleo/data.html>). The lower two units (fluvial, coastal), obscured by gas except near paleo-channel edges, exhibit a complex pattern of reflectors showing sediments prograding into (and dipping towards) the channel axis from adjacent margins. These higher acoustic impedance-contrast units represent detrital silt, sand, gravel, and woody debris eroded from nearby pre-Holocene terraces and deposited in the main channel in fluvial and coastal environments between ~15 and 7.6 ka. The third, topmost unit (estuarine) is weakly stratified and, where gas is absent, appears acoustically transparent.

[5] MS decreases sharply across stratigraphic transitions in all regions and the nearly synchronous decrease to values <6 SI units (Figure 2) indicates slower sedimentation and deposition of deeper water estuarine clays and silts as shorelines transgressed landward from the channel axis. Diagnostic environmental indicators plotted against MS in Figure 2 include fluvial (freshwater algae, mollusks, ostrac-

¹U.S. Geological Survey, Reston, Virginia, USA.

²Naval Research Laboratory, Washington, D. C., USA.

³Department of Geological Sciences, University of South Carolina, Columbia, South Carolina, USA.

⁴Maryland Geological Survey, Baltimore, Maryland, USA.

⁵U.S. Geological Survey, Woods Hole, Massachusetts, USA.

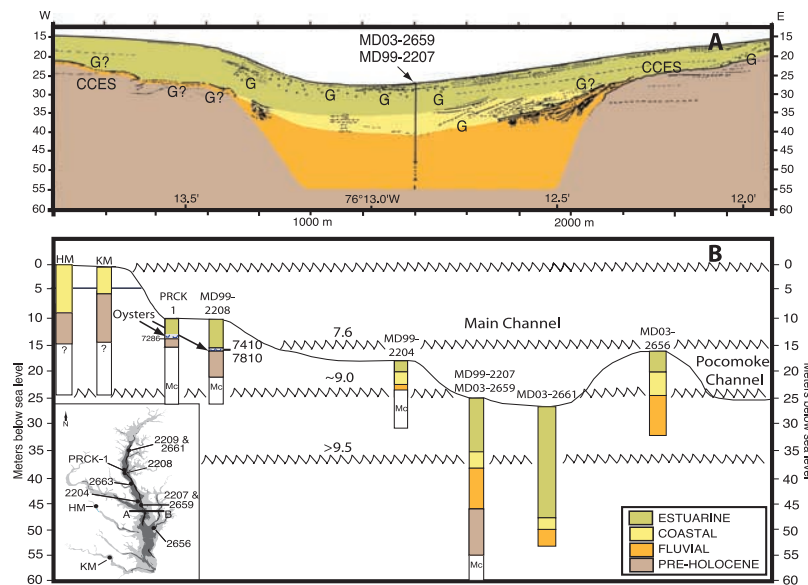


Figure 1. (a) Geophysical CHIRP line C7 ($38^{\circ}01.84'N$) off mouth of Potomac River is typical Holocene sequence in main Chesapeake Bay channel. G is gas; CCES is the Cape Charles Erosion Surface. Approx. location of MD99-2207, 03-2659 shown. (b) Stratigraphy of early Holocene marine transgression seen in fluvial, coastal, estuarine facies in Chesapeake cores projected onto a west-east transect. PRCK-1 and MD99-2208 contain ~ 7.6 ka oysters; Hunters and Kenyon marshes (HM, KM) contain late Holocene sea level records. Chronology from ^{14}C dates (auxiliary material; Figures 2 and 3) and pollen stratigraphy oak ($10.6 \text{ ka} \pm 300 \text{ yr}$), hickory ($9.4 \text{ ka} \pm 200 \text{ yr}$), hemlock declining ($5.4 \text{ ka} \pm 100 \text{ yr}$). Approximate sea level positions >9.5 , 9.0 , 7.6 ka shown, uncorrected for isostatic adjustment. Inset shows location of *Marion-Dufresne* core sites from 1999 and 2003 IMAGES cruises.

odes), coastal marsh (brackish foraminifera, ostracodes), and estuarine and marine species. The first evidence for marine incursion consists of the appearance of brackish-marine species in unit 2 are dated at ~ 9.5 ka or older in the deep channel, at ~ 9 ka in Pocomoke Sound (marsh facies), and at ~ 7.6 ka along the western margin (oyster facies). The final flooding of the bay (topmost unit) and beginning of full estuarine circulation (high salinity, deeper water) is dated at $7,601 \text{ yr}$ ($n = 8$, $2 \sigma = 49 \text{ yr}$) in five cores and marked by the permanent decrease in MS, the fall in grass and sedge pollen, and appearance of marine microfaunas.

3. Comparison to Sea Level Records and ICE-5G Model

[6] We constructed a conventional sea level curve corrected for 1 mm yr^{-1} of GIA and crosschecked it against curves for Barbados [Fairbanks, 1989], Huon Peninsula [Ota and Chappell, 1999], and Tahiti [Bard et al., 1996] coral records, and the Red Sea foraminiferal $\delta^{18}O$ record [Siddall et al., 2003] (Figure 3). Only CB samples from coastal facies (marsh, oysters) were used. All curves fit within a qualitatively defined first-order sea level envelope accounted for by uncertainty arising from coral depth habitats, vertical tectonic movements, isotopic calibration, and other processes. In addition, corrected sea level datums at $-17 \pm 1 \text{ mbsl}$ (MD03-2656, $\sim 9.2\text{--}9.0 \text{ ka}$) and -10 mbsl (MD99-2208, $\sim 7.6 \text{ ka}$) are only slightly higher than global sea level positions at -20 to -21 mbsl at 9 ka and -8 mbsl at 7.6 ka predicted by the ICE-5G eustatic model [Peltier, 2004]. Given GIA uncertainty due to shelf effects, mantle viscosity, and ice sheet thickness and location, these results

support the ICE-5G model for regional, post-glacial GIA rate $\sim 1 \text{ mm yr}^{-1}$ and mean sea level rise rates of $\sim 8\text{--}10 \text{ mm yr}^{-1}$ from 9.5 to 7.5 ka .

4. Correlation to Paleoclimate Records

[7] In order to compare the timing of sea level rise with associated climate events, we constructed a stratigraphic record of sea level from MD03-2656 using benthic foraminifers, ostracodes, pollen of coastal grasses and sedges, stable isotopes on benthic foraminifera ($\delta^{18}O_{\text{foram}}$) as paleo-sea level indicators. Figure 4 plots this record against the GISP2 ice core accumulation rate (a temperature proxy) [Cuffey and Clow, 1997] and subpolar N. Atlantic core MD99-2251 planktonic foraminiferal oxygen isotopes ($\delta^{18}O$) and sortable silt (sea-surface temperature and AMOC proxies) [Ellison et al., 2006]. The MD03-2656 sequence consists of organic-rich sediments deposited in a coastal marsh complex, including wetland, tidal channel, and sub-tidal environments. During rising sea level, coastal marshes accrete vertically at rates of ~ 1 to 7 mm yr^{-1} depending on sediment supply, vegetation, tidal range, geomorphology and other factors but, like coral reefs, rapid sea level rise can drown marshes [e.g., Belknap and Kraft, 1977].

[8] IN MD03-2656, marsh accretion indicated by several proxies began $\sim 9 \text{ ka}$ coincident with a series of peaks in ice accumulation in Greenland, and strong AMOC in the North Atlantic. During this time, the rate of marsh accretion was $2\text{--}3 \text{ mm yr}^{-1}$, suggesting a relatively slow, steady rate of sea level rise. Two periods of marsh drowning are evident. The first began at $\sim 8.9\text{--}8.8 \text{ ka}$ and is marked by an abrupt shift in dominance from marsh species to *Elphidium*, a

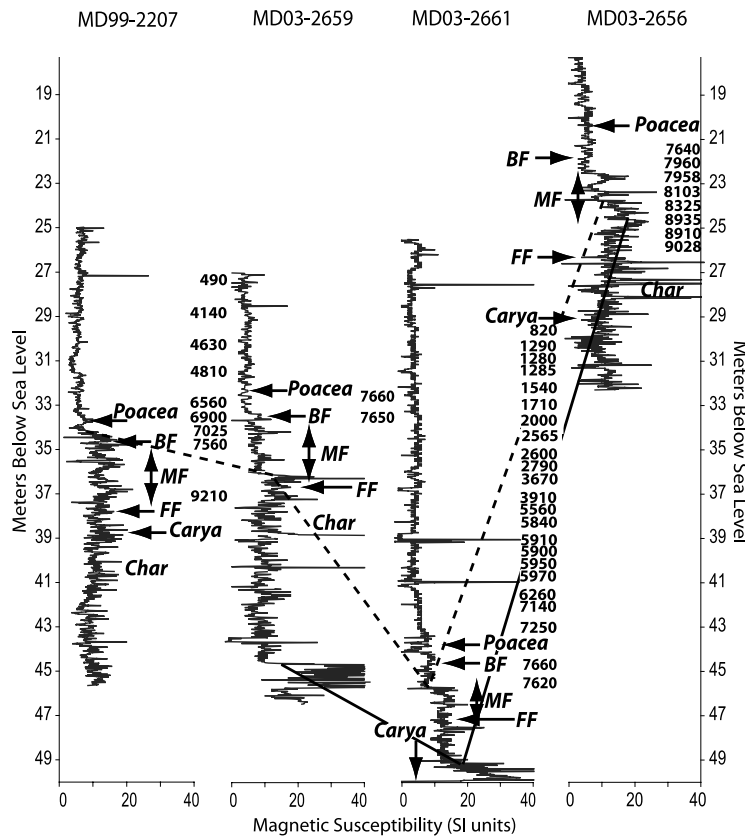


Figure 2. Early Holocene sea level rise seen in Magnetic Susceptibility (MS, SI units $\times 10^{-5}$) and micropaleontology in Pocomoke Sound (MD03-2656) and Chesapeake Bay (MD99-2207, MD03-2659, MD03-2661). Pre-Holocene MS ≥ 20 , fluvial-coastal MS = 8–20, estuarine MS = 4–6. FF, first foraminifers; BF, first marine foram *Buccella frigida*; MF, marsh foraminifera zone (*Aerenoporella*); Char, Charophytes (fresh-water algae); first *Carya* (9.4 ka \pm 200 yr, Hickory); last Poaceae (grasses) pollen (data at <http://www.ncdc.noaa.gov/paleo/data.html>). ~ 7.6 ka marks age of final flooding and inception of deep estuarine circulation. See auxiliary material for ^{14}C dates.

decrease in grass and sedge pollen, and a $\sim 1.4\%$ enrichment in $\delta^{18}\text{O}_{\text{foram}}$ equivalent to a salinity increase of ~ 8 ppt [Cronin et al., 2005]. These changes are interpreted as signifying a period of RSL rise too fast for marsh growth to keep up. Two radiocarbon dates at 760–700 cm MD03-

2656 core depth bracket the age of this zone at 8.9 to 8.3 ka. By ~ 8.3 ka, about 100–300 years after the initial pulse of freshwater from Lake Agassiz-Ojibway, there is a return to marsh-dominated faunas, an increase in grass and sedge

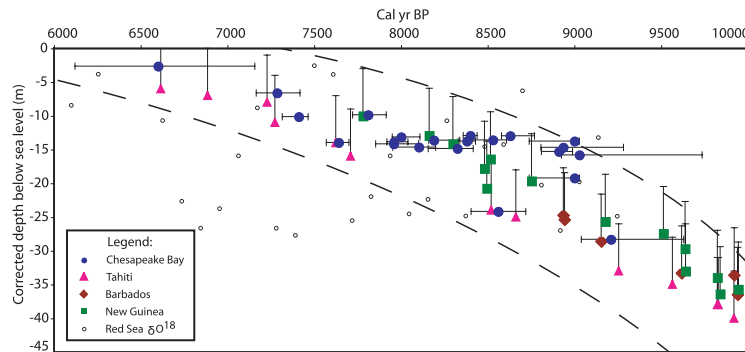


Figure 3. Chesapeake sea level curve compared to those from Tahiti [Bard et al., 1996], Barbados [Fairbanks, 1989; Fairbanks et al., 2005], and New Guinea [Ota and Chappell, 1999], all corrected for tectonic and isostatic adjustment; and isotopically-derived sea level from Red Sea isotope record [Siddall et al., 2003]. Horizontal bars signify 2- σ age range for CB samples. Vertical bars represent coral depth range (7 m), CB marsh and oyster facies (1–2 meters \approx thickness of the symbol), Red Sea isotopic uncertainty ± 12 m not shown for clarity. Dashed lines qualitatively bracket first-order sea level curve.

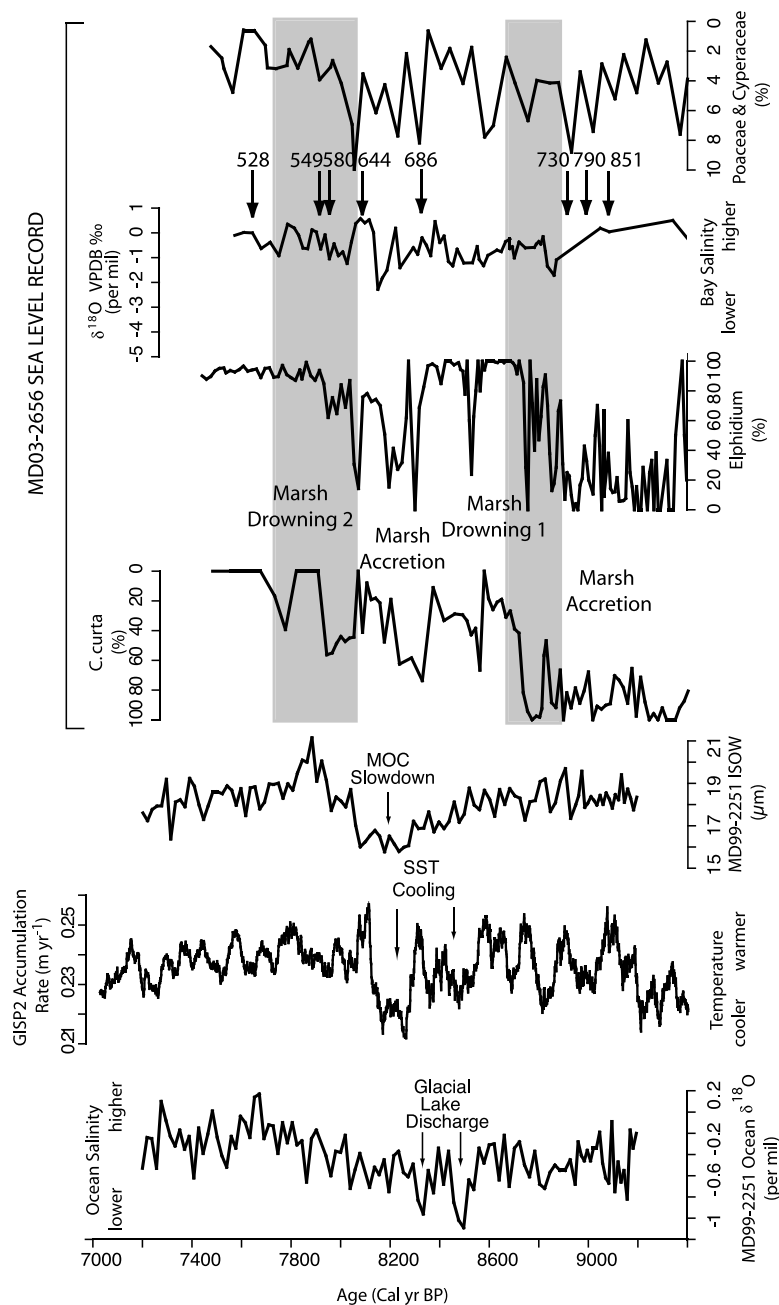


Figure 4. Comparison of Chesapeake MD03-2656 record (1050 and 450 cm) of early Holocene RSL record with North Atlantic MD03-2251 record of sea-surface salinity (SSS, $\delta^{18}\text{O}$) and sortable silt, a proxy for deep-water currents and meridional overturning circulation [Ellison *et al.*, 2006], and Greenland GISP2 ice-core accumulation rates, a proxy for atmospheric temperature [Cuffey and Clow, 1997]. Sea-surface salinity drops ~ 8.5 and 8.3 ka reflect catastrophic glacial lake drainage from North America [Barber *et al.*, 1999]. Arrows show position and core depths of radiocarbon dates (Figure 2). MD03-2656 proxies for low salinity, marsh (high salinity, drowned marsh) environments include dominant (rare) *Cytheromorpha curta*, *Aerenoporella*, rare (dominant) *Elphidium*, more (less) common grass (Poaceae) and sedge (Cyperaceae) pollen and more negative (positive) $\delta^{18}\text{O}_{\text{Elphidium}}$. Two periods of marsh accretion are each followed by rapid drowning and increased salinity during sea level rise, lagging periods of reduced SSS and MOC and atmospheric cooling by several centuries. Interval prior to 9 ka has larger age uncertainty. MD03-2656 data available at World Data Center for Paleoclimatology (<http://www.ncdc.noaa.gov/paleo/paleo.html>).

pollen, and a 2‰ depletion in $\delta^{18}\text{O}_{\text{foram}}$, all suggesting a temporary decrease in the rate of RSL rise.

[9] The second marsh drowning shows similar faunal, floral and isotopic changes signaling the inception of full

estuarine circulation and final flooding of the bay about 7.6 ka as discussed above. The age of this flooding is constrained by MD03-2656 shell (2σ age range: 8417–8158 yrs and 8200–7953 yr) and seed $^{14}\text{C}_{\text{cal}}$ ages (~ 8330 –

8150 yr, 644 cm), ~ 23 mbsl uncorrected depth and oysters (7465–7316, 7915–7721 yr) ~ 17.5 mbsl from core MD99-2208 on the western side of the bay (Figure 1b). We estimate that sea level rose ~ 6 m in 500 years or less (mean rate of 12 mm yr^{-1}). The timing of this event coincides with the “climate overshoot” described by *Ellison et al.* [2006] at 7.9 ka when resumption of vigorous meridional circulation followed the 8.6–8.2 ka cooling.

5. Discussion

[10] Additional research is needed to better constrain the timing of the final stages of deglaciation during the early Holocene, but at present, we can identify several potential meltwater sources that might have contributed. The Laurentide Ice Sheet was still retreating ~ 9.5 – 9.0 ka [*Dyke et al.*, 2003], and it is considered a meltwater source at this time in the ICE-5G model. Evidence also exists for an atmospheric climatic optimum in Antarctica ~ 11.5 – 9.0 ka [*Masson et al.*, 2000], and Antarctic ice may also have contributed. For the rapid RSL event at 8.2– 7.6 ka, the volume of water draining from glacial Lake Agassiz-Ojibway can only account for ~ 0.4 to 1.2 m of sea level rise [*Törnqvist et al.*, 2004], which means the rest must have come from accelerated melting of land-based ice. Glacial evidence suggests that most northern hemisphere LGM-age ice had melted by ~ 8.5 – 8.0 ka, and Antarctica is a more likely source of meltwater at this time. This idea is consistent with evidence for ice-shelf collapse and deglaciation of some marine-based sectors of the Antarctic ice sheet during the early Holocene [*Ingólfsson and Hjort*, 1999; *Bentley et al.*, 2005]. One mechanism to explain rapid sea level rise involves the strengthening of North Atlantic Deep Water ~ 7.9 ka which might destabilize ice shelves along Antarctic margins through its influence on Southern Hemisphere Circumpolar Deep Water as proposed for Dansgaard-Oeschger events during the last glacial period [*Kanfoush et al.*, 2000]. Ice-shelf destabilization supports the idea of inter-hemispheric asymmetry in which Southern Hemisphere climate and ice sheet responds to Northern Hemisphere fresh-water forcing of AMOC. However, the exact timing of Antarctic ice sheet decay varies by region, precluding a simple correlation of glaciological events with sea level. Regardless of the direct causes, the high rate of sea level rise suggests rapid destabilization of sectors of remaining ice sheets at the end of the last deglaciation.

[11] **Acknowledgments.** We thank captains and crews of the *R/V Kerhin* and *Marion-Dufresne*, and the IMAGES program, L. Labeyrie, E. Michel, C. Laj, and Y. Balut for coring assistance. Helpful comments from H. Dowsett, J. Self-Trail, W. Ruddiman, V. Masson-Delmotte, and I. Winograd improved the manuscript. We appreciate U-series analyses from C. Hillaire-Marcel and B. Ghaleb, mollusk IDs from R. Lockwood and L. Wingard, sea-level data from E. Bard and R. Fairbanks, input on 1999 cores from J. King and C. Heil. Cronin, Willard, Thunell, Berke supported by USGS Earth Surface Dynamics Program; Vogt and Pohlman by Office of Naval Research; Halka by MGS. Some ^{14}C dates from National Ocean Sciences Accelerator Mass Spectrometry Facility, Woods Hole Oceanographic Institution.

References

Alley, R. B., et al. (1997), Holocene climate instability: A large event 8000–8400 years ago, *Geology*, *25*, 482–486.
Alley, R. B., P. U. Clark, P. Huybrechts, and I. Joughin (2005), Ice-sheet and sea-level changes, *Science*, *310*, 456–460.

Barber, D. C., et al. (1999), Forcing of the cold event of 8,200 years ago by catastrophic drainage of Laurentide lakes, *Nature*, *400*, 344–348.
Bard, E., B. Hamelin, M. Arnold, L. Montaggioni, G. Cabioch, G. Faure, and F. Rougerie (1996), Deglacial sea-level record from Tahiti corals and the timing of global meltwater discharge, *Nature*, *382*, 241–244.
Belknap, D. F., and J. C. Kraft (1977), Holocene relative sea-level changes and coastal stratigraphic units on the northwest flank of the Baltimore Canyon trough geosyncline, *J. Sediment. Petrol.*, *47*, 610–629.
Bentley, M. J., et al. (2005), Early Holocene retreat of the George VI ice shelf, Antarctic Peninsula, *Geology*, *33*, 173–176.
Colman, S. M., J. Halka, C. Hobbs III, R. Mixon, and D. Foster (1990), Ancient channels of the Susquehanna River beneath Chesapeake Bay and the Delmarva Peninsula, *Geol. Soc. Am. Bull.*, *102*, 1268–1279.
Cronin, T. M. (Ed.) (2000), Initial report on IMAGES V cruise of the *Marion-Dufresne* to the Chesapeake Bay, June 20–22, 1999, *U.S. Geol. Surv. Open File Rep.*, *00-306*, 1–133.
Cronin, T. M., R. Thunell, G. S. Dwyer, C. Saenger, M. E. Mann, C. Vann, and R. R. Seal II (2005), Multiproxy evidence of Holocene climate variability from estuarine sediments, eastern North America, *Paleoceanography*, *20*, PA4006, doi:10.1029/2005PA001145.
Cuffey, K. M., and G. D. Clow (1997), Temperature, accumulation, and ice sheet elevation in central Greenland through the last deglacial transition, *J. Geophys. Res.*, *102*, 26,383–26,396.
Dyke, A. S., A. Moore, and L. Robertson (2003), Deglaciation of North America, *Geol. Surv. Can. Tech. Rep. Open File*, *1574*.
Ellison, C. R. W., M. R. Chapman, and I. R. Hall (2006), Surface and deep ocean interactions during the cold climate event 8200 years ago, *Science*, *312*, 1929–1932.
Fairbanks, R. A. (1989), 17,000-year glacio-eustatic sea level record: Influence of glacial melting rates on the Younger Dryas event and deep-ocean circulation, *Nature*, *342*, 637–641.
Fairbanks, R. G., et al. (2005), Radiocarbon calibration curve spanning 0 to 50,000 years BP based on paired $^{230}\text{Th}/^{234}\text{U}/^{238}\text{U}$ and ^{14}C dates on pristine corals, *Quat. Sci. Rev.*, *24*, 1781–1796.
Haug, G. H., K. A. Hughen, L. C. Peterson, D. M. Sigman, and U. Röhl (2001), Southward migration of the Intertropical Convergence Zone through the Holocene, *Science*, *293*, 1304–1308.
Howat, I. M., I. Joughin, and T. A. Scambos (2007), Rapid changes in ice discharge from Greenland outlet glaciers, *Science*, *315*, 1559–1561.
Ingólfsson, O., and C. Hjort (1999), The Antarctic contribution to Holocene global sea level rise, *Polar Res.*, *18*(2), 323–330.
Kanfoush, S. L., D. A. Hodell, C. D. Charles, T. P. Guilderson, P. G. Mortyn, and U. S. Ninnemann (2000), Millennial-scale instability of the Antarctic ice sheet during the last glaciation, *Science*, *288*, 1815–1818.
Laj, C. (Ed.) (2005), MD132 P. I. C. A. S. O. IMAGES XI cruise report, *Rep. OCE/2004/02*, Inst. Polaire Français, Plouzané, France.
Masson, V., et al. (2000), Holocene climate variability in Antarctica based on 11 ice-core isotopic records, *Quat. Res.*, *54*, 348–358.
Miller, L., and B. C. Douglas (2004), Mass and volume contributions to twentieth-century global sea level rise, *Nature*, *428*, 406–409.
Ota, Y., and J. Chappell (1999), Holocene sea-level rise and coral reef growth on a tectonically rising coast: Huon Peninsula, Papua New Guinea, *Quat. Int.*, *55*, 51–59.
Peltier, W. R. (1996), Global sea level rise and glacial isostatic adjustment: An analysis of data from east coast of North America, *Geophys. Res. Lett.*, *23*, 717–720.
Peltier, W. R. (2004), Global glacial isostasy and the surface of the ice-age earth: The ICE-5G (VM2) model and GRACE, *Ann. Rev. Earth Planet. Sci.*, *32*, 11–149.
Rohling, E. J., and H. Pälike (2005), Centennial-scale climate cooling with a sudden cold event around 8,200 years ago, *Nature*, *434*, 975–979.
Shepherd, A., and D. Wingham (2007), Recent sea-level contributions of the Antarctic and Greenland ice sheets, *Science*, *315*, 1529–1532.
Siddall, M., et al. (2003), Sea-level fluctuations during the last glacial cycle, *Nature*, *423*, 853–858.
Teller, J. T., D. Leverington, and J. Mann (2002), Freshwater outbursts to the oceans from glacial Lake Agassiz and their role in climate change during the last deglaciation, *Quat. Sci. Rev.*, *21*, 879–887.
Törnqvist, T. E., S. J. Bick, J. L. González, K. van der Borg, and A. F. M. de Jong (2004), Tracking the sea-level signature of the 8.2 ka cooling event: New constraints from the Mississippi Delta, *Geophys. Res. Lett.*, *31*, L23309, doi:10.1029/2004GL021429.
Truffer, M., and M. Fahnstock (2007), Rethinking ice sheet time scales, *Science*, *315*, 1508–1510.
Vogt, P. R., M. Czarniecki, and J. P. Halka (2000), *Marion-Dufresne* coring in Chesapeake Bay: Geophysical environment at sites MD99-2204 and 2207, in *Initial report on IMAGES V cruise of the Marion-Dufresne to the Chesapeake Bay, June 20–22, 1999*, edited by T. M. Cronin, *U.S. Geol. Surv. Open File Rep.*, *00-306*, 32–39.

Willard, D. A., C. E. Bernhardt, D. A. Korejwo, and S. R. Meyers (2005), Impact of millennial scale climate variability on eastern North American terrestrial ecosystems: Pollen-based reconstructions, *Global Planet. Change*, 47, 17–35.

M. Berke, T. M. Cronin, and D. A. Willard, U. S. Geological Survey, 926a National Center USGS, 1220 Sunrise Valley Drive, Reston, VA 20192, USA. (tcronin@usgs.gov)

J. Halka, Maryland Geological Survey, 2300 Saint Paul Street, Baltimore, MD 21218, USA.

J. Pohlman, U. S. Geological Survey, 384 Woods Hole Road, Woods Hole, MA 02543, USA.

R. Thunell, Department of Geological Sciences, University of South Carolina, 701 Sumter Street, EWSC Room 617, Columbia, SC 29208, USA.

P. R. Vogt, Naval Research Laboratory, 4555 Overlook Avenue SW, Washington, DC 20375, USA.